

Article

A Framework to Assess and Analyze Enhancement Options for Microgrid Resiliency against Extreme Wind

Rajesh Karki *  and Binamra Adhikari

Department of Electrical & Computer Engineering, University of Saskatchewan, Saskatoon, SK S7N 5A9, Canada; binamra.adhikari@usask.ca

* Correspondence: rajesh.karki@usask.ca

Abstract: The objective of a power system is to provide electricity to its customers as economically as possible with an acceptable level of reliability while safeguarding the environment. Power system reliability assessments are routinely performed to ensure adequate system resources and reliable operation using well-established methods, quantitative metrics, regulatory standards and compliance incentives in the jurisdictions of responsibilities. The alarming increase in the occurrence of extreme events, which are not included in routine reliability evaluation, has raised growing concerns due to the catastrophic impacts of these events on distribution systems. The potential economic losses due to prolonged and large-scale outages have motivated utility planners, operators and policy makers to acknowledge the importance of system resiliency against such events. Power system resiliency, however, lacks widely accepted modeling frameworks, standards, assessment methods and metrics. This paper presents a resilience assessment framework, along with quantifiable metrics to assess the resiliency of a distribution system against extreme winds, which are among the most common form of natural disasters affecting the North American region. The paper assesses the effectiveness of infrastructural and operational resilience enhancement strategies. The effectiveness of preventive and corrective strategies is also analyzed on a test distribution system.

Keywords: DERs; resiliency; infrastructural strategies; pole hardening; extreme wind



Citation: Karki, R.; Adhikari, B. A Framework to Assess and Analyze Enhancement Options for Microgrid Resiliency against Extreme Wind. *Energies* **2024**, *17*, 2573. <https://doi.org/10.3390/en17112573>

Academic Editor: Om P. Malik

Received: 26 March 2024

Revised: 14 May 2024

Accepted: 15 May 2024

Published: 26 May 2024



Copyright: © 2024 by the authors. Licensee MDPI, Basel, Switzerland. This article is an open access article distributed under the terms and conditions of the Creative Commons Attribution (CC BY) license (<https://creativecommons.org/licenses/by/4.0/>).

1. Introduction

The conventional distribution system fed from a centralized power supply system is rapidly transforming into a decentralized and relatively independent network structure with increasing penetrations of distribution energy resources (DERs). The evolving infrastructure of distribution systems is exposed to considerable increase in man-made extreme events, such as cyber-attacks, and natural disasters such as earthquakes, hurricanes/tornadoes, floods, ice storms, extreme winds [1], etc., that cause prolonged and/or wide-scale power outages. The impact of the different types of extreme events on the distribution system and the subsequent recovery methods are very specific to the type of extreme event. Extreme winds are known to affect distribution systems the most due to their topological and operational characteristics [2] and are therefore the subject of this research. Although underground cables commonly exist in urban distribution systems, a notable portion of the system is overhead infrastructure. Rural distribution systems are mostly overhead due to cost constraints, and are exposed to extreme weather conditions. The distribution network succumbing to extreme winds sustains considerable damage to the infrastructures and often requires lengthy and costly restoration processes, but are not accounted for by established reliability guidelines. Existing approaches to planning a reliable distribution system account for random component outages, generation variations, load uncertainties and the capability of the distribution network to satisfy the customer demands, but do not incorporate high impact low probability (HILP) events in routine applications. The need to address such concerns has contributed to loaning resiliency concepts

from other fields of studies. One of the early sightings of resiliency is found in the field of ecology in [3], where the author defines resiliency as the measure of persistence of a system and of its ability to absorb change and disturbance and still maintain the same relationship between population and state variables. The concept of resiliency has been interpreted from different perspectives in different fields of study, but the overarching concept has remained the same. Resiliency is concerned with the impact on the system due to rare events, and the ability of the system to absorb and recover from them. In power systems, the proliferated exposure of distribution systems to extreme events has emphasized the importance of resiliency studies. The impending degradation of structural integrity and the potential magnitude of economic losses due to such damages and power outages have highlighted the need for resilient distribution systems. Power system resiliency studies, however, do not yet have established frameworks, metrics and regulatory standards that are widely accepted by the electric utilities [4]. Moreover, ambiguous approaches in envisioning a resilient grid are bringing surging concerns about the authenticity and credibility of the applications of such approaches.

A limited amount of literature can be found on power system resilience against extreme winds. Min Ouyang et al. [5] provide a realistic fragility model to assess resiliency using percentage of load connected. H. Gao et al. [6] provide an effective optimization algorithm that maximizes the service time of critical loads. The authors of [7] found that a significant improvement in resiliency can be made with the help of microgrids. Efficient automated switching for microgrids/DERs operations are proposed in [8] and tested on a 34-bus and 123-bus system. The authors of [9–11] model extreme wind on a bulk system. An infrastructure-based resilience assessment was done assessing the status of infrastructures after an event in [8], in comparison with [10,11] which use EENS to calculate resiliency. S. Yao et al. [12] validate the efficient approach of graph theory in modelling a distribution network and show that microgrids can be used to ensure a flexible and resilient distribution network. An effective crew management strategy to ensure a resilient distribution system is demonstrated by [13] on the IEEE-34 bus. W. Yuan et al. [14] include the geographical extensivity of extreme wind in their study. Optimal restorations of distribution grids considering the switching operations and DERs/microgrids in the aftermath of extreme wind are proposed in [6,9,12,15–20].

M Panteli et al. [9] propose a resilience index called $\Phi\Delta\text{EPI}$ (pronounced as “flep”) to assess the degradation of a power system following an extreme event. Chanda, S. et al. [21] use a simulation-based method to quantify resiliency and also identify the improvements using microgrids and DERs. Gautam, P. et al. [22] quantify the resilience of a distribution network using three metrics, namely the expected probability of interruption, expected outage duration and expected energy not served during the extreme event. Their resilience evaluation framework embedded a wind-induced extreme-event-generating model, damage assessment model and an optimal restoration model utilizing DER. Bie et al. [23] present an in-depth discussion on the effectiveness of the proposed load restoration framework in creating a resilient grid.

A considerable amount of literature is present on the judicious utilization of DERs/microgrids and their switching operations to ensure the critical load points are restored quickly. However, ambiguity in the identification of infrastructural and operational measures to ensure resiliency in the distribution system and lack of information on the appropriate steps to implement remedial measures in the planning and operating phases are observed in much of the literature. The impact of transmission line fragility on the resiliency of the distribution network is also an important aspect not yet investigated, as the resiliency of a distribution system cannot be guaranteed without a resilient delivery network feeding the system.

System resilience evaluation methods should have the ability to incorporate the uncertainties and correlations in the performance of different type of strategies for improving resilience. They should be able to identify between an infrastructural and operational strategy and assess the worth of the strategies in order to make proper investment decisions. It

is extremely difficult to encompass all of these factors into an analytical model and validate them. A sequential Monte Carlo simulation (MCS) can be used to observe the behavior of the system chronologically throughout the period of study, but it becomes computationally burdensome due to the need to employ large simulation samples and carry out load flow and optimization algorithms for each simulated event. This paper presents the development of a novel resilience evaluation framework including a probabilistic extreme event model, resilience enhancement model and resilience assessment model incorporating infrastructural and operational strategies, and integrates them using a MCS framework that preserves relevant time-varying dependencies of the various stochastic parameters in the system. A non-sequential MCS is chosen over sequential MCS for computational efficiency.

Infrastructural strategies, such as pole hardening, are modelled with the help of fragility curves [11]. Its impact on the distribution system is studied using the proposed resilience assessment model. The resilience assessment model observes the load supplied before, during and after an extreme event and creates a load profile to quantify its resiliency. The availability of repair personnel and its impact on the resiliency of the distribution system is also evaluated using the proposed framework. The application of DERs is also facilitated and studied in the proposed resilience assessment framework. A graph-theory-based search algorithm is used to find the affected load points and identify segments that can operate under islanded microgrid mode. An optimization problem based on mixed integer linear programming (MILP) is formulated to minimize the energy curtailment due to outages.

This paper presents a novel resiliency assessment framework against extreme winds and applies the proposed framework to explore various resiliency enhancement strategies. This paper also illustrates a method of coordinating transmission infrastructure resilience with distribution system resiliency enhancement strategies by providing comparative quantitative indicators. The main contribution of this paper is summarised below:

1. To develop a quantitative framework to assess distribution system resilience that incorporates extreme wind modeling, conditional impact assessment of extreme wind considering operational constraints/conditions and modeling restorative actions to obtain expected resilience indices.
2. To apply the proposed resilience framework to quantify the benefits of infrastructure hardening, impact management using DERs and restorative strategies.
3. To provide a methodology to coordinate transmission infrastructure enforcement with distribution resilience enhancement and carry out comparative studies for investment decisions.

2. Methodology

The development of the proposed distribution system resiliency assessment framework is presented in this section. The framework is based on the system response curve shown in Figure 1, which is also known as a resilience trapezoid [1]. On the x-axis of Figure 1, t_0 represents the time before the occurrence of the extreme wind when the system is working under normal conditions. The extreme wind event starts at time t_{se} , and the impact begins to change the operating condition of the system. This is designated as Phase I in Figure 1. Extreme wind can tear down poles and damage overhead lines and outdoor equipment, causing load loss in the system. This increasing load loss, or infrastructural damage caused by the extreme wind, is represented by the drop in resilience levels between times t_{se} and t_{ee} ; the latter represents the end of the extreme wind event. Phase II or post-disturbance degraded state represents the time interval after the extreme wind subsides and before the restorative measures are deployed. At this phase, the operators start assessing the damage in order to decide how to restore the supply to the critical and other loads in the affected areas. This requires identification and assessment of the problem and planning of restoration measures in order to minimize losses.

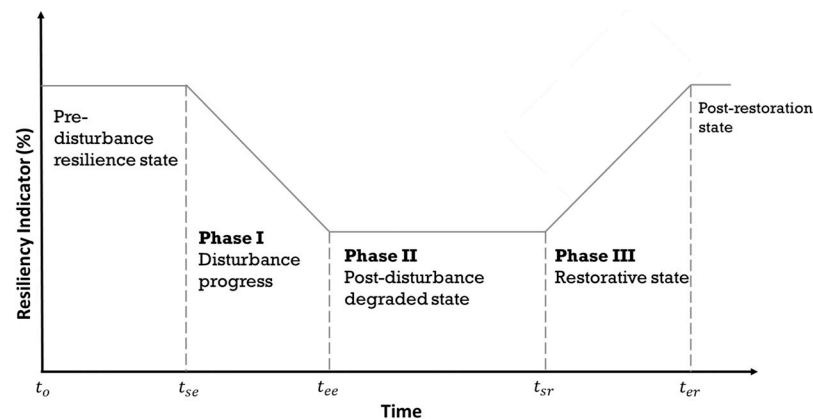


Figure 1. Typical resilience trapezoid.

Restorative actions can include deployment of DERs to supply the loads and deployment of crewmen to repair damaged poles, lines and related equipment. These actions gradually restore service to the curtailed loads, which translates to a decrease in load loss and an increase in the resilience level as shown by the positive slope in Phase III of the figure. Phase III, or the restorative state, is the time interval between t_{sr} , the start of restorative actions, and t_{er} , the end of the restorative actions.

The resiliency of a system can be improved through different strategies. Each of these measures produces a different response in the system. Therefore, in order to provide the distinction, the strategies are categorized into two types: (i) long-term infrastructural planning, and (ii) short-term operational strategies. Pole hardening (using stronger materials to increase the strength of poles) and under-grounding cables are some of the long-term preventive strategies to achieve a resilient grid against extreme wind. These strategies can be relatively costly and are to be decided during the planning phase but provide proactive solutions to the problem. Investment in DERs is another example of long-term infrastructural planning. Short-term operational strategies include strategies like deployment of crewmen, efficient operation/management of DERs, etc. These strategies provide corrective action and reduce the outage time due to extreme wind.

Each of these strategies reacts differently and therefore produces different results in the distribution system resilience enhancement. This paper, therefore, models and studies each strategy independently. A quantitative assessment of resilience is done for each study after the associated changes are made in the distribution system. The system resilience profile is studied for improvement or degradation, and conclusions are drawn on the effectiveness of the strategies using appropriate quantitative indices. The following subsection describes the main steps involved in modelling the wind and the system responses, and the impact on the distribution system incorporating the remedial strategies. The proposed indices are used to assess the effectiveness of the strategies.

2.1. Extreme Wind Modelling

Different approaches have been used to model wind speed characteristics. Ref. [24] discusses the advantages and disadvantages of the various methods including the TimeGAN model that relies hugely on the available dataset size for the prediction of wind speed. Comprehending the limitations of such methods due to historical rarity, this paper employs a statistical model described in this section. The “duration” of the event and the “profile” of the wind speed during the event are the two key mathematical features considered in extreme wind modeling. The “duration” refers to the time span of the extreme wind. It can range from a few hours to a few days. This paper models the duration using exponential approximation. Exponential distribution is approximated based on historical data of outages associated with wind events to estimate the mean duration of the outage times [25]. The data in [25] contain wind event duration for power outages associated with extreme

wind from the year 2000 to 2016. This estimation is then used to randomly generate the duration of extreme events in hours using the ‘expnd’ function in MATLAB. The “profile” represents the wind speed throughout the duration of the extreme wind event. The profile is generated using a Gumbel distribution, also known as the extreme-I distribution.

Equation (1) shows the cumulative distribution function (CDF) of the Gumbel distribution. The symbols μ and β in (1) are the location and scale parameters of the Gumbel distribution, respectively. Wind speed samples (w_n) are generated from the inverse transform of Equation (1) using MATLAB. Equation (2) shows the output of the extreme wind model. The variable n in Equation (2) is the duration in hours obtained from exponentially fitting the historical data, and w_i gives the wind speed for the i th hour of the event. The frequency and/or severity of extreme wind events are expected to increase with climate change. This effect can be timely incorporated in the above statistical model using updated wind data set obtained by replacing the oldest data from the data pool with the most recent data.

$$F(x, \mu, \beta) = e^{-e^{-\frac{x-\mu}{\beta}}} \tag{1}$$

$$W = \{w_1, w_2, \dots, w_n\} \tag{2}$$

2.2. Impact Assessment on the Distribution System Due to an Extreme Wind Event

The distribution system components exposed to an extreme wind event can fail depending on the severity of the event and the structural fragility of the elements. A generic structural fragility of a distribution pole is shown in Figure 2. This figure is mathematically expressed by the empirical Equation (3), which is utilized to evaluate the failure probability of distribution poles FP_{pl} . These values are then used to calculate the failure probability of line segments, FP_{ij} , using Equation (4). The variable pl represents a pole, and ij represents the line segment between bus i and bus j , respectively.

$$FP_{pl} = 0.0001 \times \exp[0.0421 \times V_w] \tag{3}$$

$$FP_{ij} = 1 - \prod_{pl=1}^{NP_{pl}} (1 - FP_{pl}) \tag{4}$$

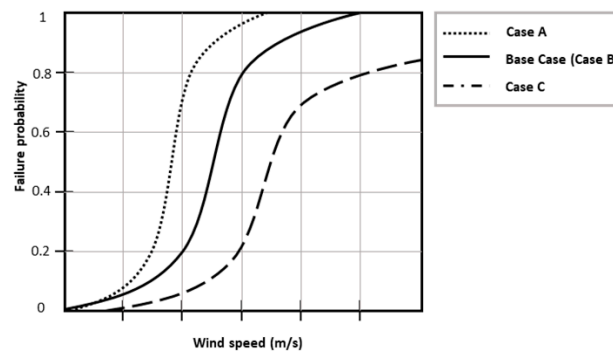


Figure 2. Fragility curve for distribution and transmission network.

The failure status for each line segment of the distribution system is then determined using uniform random numbers. The random number x_{line} is compared with probability of failure of each line segment obtained from Equations (3) and (4). The status of individual line segment is then evaluated using Equation (5).

$$\gamma_{ij}^{line} = \begin{cases} 1; & \text{if } x_{line}(= \cup(0,1)) \leq FP_{ij} \\ 0; & \text{otherwise} \end{cases} \tag{5}$$

The information is then utilized to identify the unhealthy and healthy sections of the distribution grid. A depth-first search (DFS) algorithm, based on graph theory [22] is used in this paper to assess the load points affected after an extreme event and identify the healthy and unhealthy sections of the network. The information regarding the status of the distribution system elements is provided by the DFS. After an extreme event, the load points may reside in one of the following three states: (i) grid-connected mode, (ii) islanded mode, and (iii) failed mode. The main utility supplies the segment in the grid-connected mode. The healthy part of the network is supplied by DERs in the islanded mode. In the failed mode, the load point is not supplied by the main grid or DERs. It is assumed that fully reliable circuit breakers/reclosers are equipped with sectionalizers on both sides for fault isolation.

2.3. Restoration Mechanism following an Extreme Event

This section describes the restoration mechanism of the distribution system after an extreme event. Restoration mechanism depends on the state of the system, available resources and the restoration strategy decided for implementation. Preventive strategy and the corrective strategy are two strategies studied in this paper. Preventive strategy aims to strengthen the system such that it rides through an extreme wind with minimal or no damages. Corrective strategy aims to provide measures to mitigate losses by managing and deploying operational resources at the time of an extreme wind. Pole hardening and investment in DERs are the long-term preventive strategies, whereas managing available DERs and deployment of repair crew are the operational corrective strategies considered in this study.

Preventive strategies can avoid or minimize damages, but may still need repair in the system. The repair takes place for the failed line segments in the system. Corrective strategies also sustain damages in the line segments and follow the same principle. Both strategies follow the same restoration mechanism. The restoration time depends on the magnitude of repair and the number of repair crew deployed. The repair times of components are assumed to be exponentially distributed. The repair time rt for a component, such as a line segment, is calculated using Equation (6), where m is the mean time to failure of the component and U is a uniformly distributed random number between 0 and 1.

$$rt = -\frac{1}{m} \ln(U) \quad (6)$$

The mean time to repair is based on one member of repair personnel being deployed for the repair of a faulty line segment. The restoration time is then calculated based on repair time of individual segments, number of line segments damaged and repair personnel available as depicted in Figure 2. The variables f and rp represent number of failed segments and number of repair personnel, respectively.

The modes in which the load points reside following an extreme wind event are first identified. The load points in the islanded and failed modes need restoration. The buses connecting these load points are identified and then sorted on the basis of priority. The critical loads have priority over the non-critical loads in the restoration process. The time required to restore each bus depends on the number of load points restored. A restoration profile for each of the buses in the distribution system is obtained, which contains amount of load restored in each hour.

2.4. Modelling of Operating Strategies with DERs

This section details the MILP-based optimization problem formulated for islanded microgrids. Table 1 includes the notations used in the optimization.

Table 1. Notations used in optimization.

$i/j, ij, p, c, e, m$	Indices of bus, line section, PV, CDG, ESS and islanded microgrids, respectively
$\Omega_B, \Omega_{IJ}, \Omega_{PV}, \Omega_{CDG}, \Omega_{ESS}, \Omega_M$	Set of bus, line section, PV, CDG, ESS and islanded microgrids, respectively
t/T	Index and total estimated outage time
$pr_{CDG}, pr_{ESS}, pr_{PV}$	Operational cost of CDG, ESS and PV, respectively (\$/MWhr)
pr_i^{lc}	Penalty cost for load curtailment for load at bus i (\$/MWhr)
$LC_{a,i}(t), LC_{r,i}(t)$	Active and reactive load curtailed at bus i , time t (MW and MVAR)
$\eta_{e,i}^c, \eta_{e,i}^d$	Charging and discharging efficiency of ESS at bus i , respectively (%)
$V_i(t), \theta_i(t)$	Voltage magnitude and phase angle at bus i , time t (p.u.)
$P_{c,i}(t), Q_{c,i}(t)$	Active and reactive power from CDG at bus i , time t (MW and MVAR)
$P_{p,i}(t)$	Active power from PV at bus i , time t (MW)
$P_{ij}(t), Q_{ij}(t)$	Active and reactive power flowing between line ij at time t (MW and MVAR)
$PD_i(t), QD_i(t)$	Active and reactive power demand at bus i , time t (MW and MVAR)
$P_{e,i}^d(t), P_{e,i}^c(t)$	Discharging and charging power associated with ESS at bus i , time t (MW)
$Q_{e,i}(t)$	Reactive power from ESS at bus i , time t (MVAR)
$SOC_{e,i}(t)$	State of charge of ESS at bus i , time t (MWhr)
$\gamma_{e,i}^c(t)$	Binary variable representing charging status of ESS at bus i for period t (1 for charging, 0 otherwise)
$\gamma_{e,i}^d(t)$	Binary variable representing discharging status of ESS at bus i for period t (1 for discharging, 0 otherwise)
$\overline{P}_{p,i}(t)$	Maximum available power from PV at bus i , time t (MW)
$\overline{X}, \underline{X}$	Maximum and minimum limit of parameter X , respectively (X = active/reactive power of DERs, charging/discharging power of ESS, SOC of ESS, bus voltage magnitude/phase angle)

The implementation of DERs is based on [22]. The nodal power injected into the grid is represented by Equations (7) and (8). P , Q and ΔV , respectively, represent the column vector of active power, reactive power and the incremental voltage from the nominal value of each bus.

$$P = G' \Delta V - B' \theta \quad (7)$$

$$Q = -B'' \Delta V - G' \theta - B_{sh} \quad (8)$$

The admittance matrix is given by $Y = G + jB$, where each element in i th row and j th column is shown by $Y_{ij} = G_{ij} + jB_{ij}$. G'_{ij} , B'_{ij} , B''_{ij} and B_{sh} are obtained from Equations (9)–(12)

$$G'_{ij} = \begin{cases} -G_{ij}; & \text{if } i \neq j \\ \sum_{\substack{k \in \Omega_{BN} \\ k \neq i}} G_{ik} & \text{if } i = j \end{cases} \quad (9)$$

$$B'_{ij} = \begin{cases} -B_{ij}; & \text{if } i \neq j \\ \sum_{\substack{k \in \Omega_{BN} \\ k \neq i}} B_{ik} & \text{if } i = j \end{cases} \quad (10)$$

$$B''_{ij} = \begin{cases} -B_{ij}; & \text{if } i \neq j \\ 2B_{i0} + \sum_{\substack{k \in \Omega_{BN} \\ k \neq i}} B_{ik} & \text{if } i = j \end{cases} \quad (11)$$

$$B_{sh} = [B_{10}, B_{20}, \dots, B_{i0}, B_{NB0}]^T \quad (12)$$

where the shunt susceptance of bus i is given by B_{io} , and the set of network buses and the total number of network buses are denoted by Ω_{BN} and N_B , respectively.

An optimization problem is formed with the objective of minimizing the load curtailments over the duration of restoration time calculated from Figure 2. The objective function in Equation (13) considers the load restoration priority based on the penalty cost for the curtailment of load points.

$$\text{Min.} \sum_{t=1}^T \sum_{i \in \Omega_B} LC_{a,i}(t) \times pr_i^{lc} + P_{p,i}(t) \times pr_{CDG} + P_{e,i}(t) \times pr_{ess} + P_{c,i}(t) \times pr_{CDG} \quad (13)$$

The objective function in Equation (13) is subjected to the constraints in Equations (14)–(30), where $\forall i \in \Omega_B$, $\forall ij \in \Omega_{IJ}$, $\forall t \in T$. The multi-period AC power flow equality constraints for load balance for the islanded microgrid are given in Equations (14) and (15). The capacity constraints of line sections are described in Equations (16)–(19). Note that the linearized AC load flow equations utilized in Equations (14)–(17) are based on Equations (7)–(12). In Equations (20) and (21), the nodal voltage magnitude and phase angle constraints are detailed. The state of charge (SOC) update and minimum/maximum SOC allowed for ESS are represented in Equations (22) and (23). The charge/discharge rates of the ESS are enforced in Equations (24)–(26), where the binary variables are used to ensure ESS either charges or discharges at a time. The maximum and minimum value of active and reactive power from the conventional distributed generation (CDG), photovoltaic arrays (PV) and ESS are considered in Equations (27)–(30).

$$-P_{c,i}(t) - P_{p,i}(t) + P_{e,i}^c(t) - P_{e,i}^d(t) + \sum_{j \in \Omega_B} G'_{ij} \Delta V_j - \sum_{j \in \Omega_B} B'_{ij} \theta_j - LC_{a,i}(t) = -P_{D,i}(t) \quad (14)$$

$$-Q_{c,i}(t) - Q_{e,i}(t) - \sum_{j \in \Omega_B} B''_{ij} \Delta V_j - \sum_{j \in \Omega_B} G'_{ij} \theta_j - B_{sh_i} - LC_{r,i}(t) = -Q_{D,i}(t) \quad (15)$$

$$P_{ij}(t) = (\Delta V_i - \Delta V_j) G_{ij} - (\theta_{ij} - \theta_j) B_{ij} \quad (16)$$

$$Q_{ij}(t) = -(\Delta V_i - \Delta V_j) B_{ij} - (\theta_i - \theta_j) G_{ij} \quad (17)$$

$$\underline{P}_{ij} \leq P_{ij}(t) \leq \overline{P}_{ij} \quad (18)$$

$$\underline{Q}_{ij} \leq Q_{ij}(t) \leq \overline{Q}_{ij} \quad (19)$$

$$\underline{V}_i \leq V_i(t) \leq \overline{V}_i \quad (20)$$

$$\underline{\theta}_i \leq \theta_i(t) \leq \overline{\theta}_i \quad (21)$$

$$SOC_{e,i}(t) = SOC_{e,i}(t-1) + \eta_{e,i}^c \times P_{e,i}^c(t) - \frac{P_{e,i}^d(t)}{\eta_{e,i}^d} \quad (22)$$

$$\underline{SOC}_{e,i} \leq SOC_{e,i}(t) \leq \overline{SOC}_{e,i} \quad (23)$$

$$\gamma_{e,i}^c(t) \times \underline{P}_{e,i}^c \leq P_{e,i}^c(t) \leq \gamma_{e,i}^c(t) \times \overline{P}_{e,i}^c \quad (24)$$

$$\gamma_{e,i}^d(t) \times \underline{P}_{e,i}^d \leq P_{e,i}^d(t) \leq \gamma_{e,i}^d(t) \times \overline{P}_{e,i}^d \quad (25)$$

$$\gamma_{e,i}^c(t) + \gamma_{e,i}^d(t) \leq 1 \quad (26)$$

$$\underline{P}_{c,i} \leq P_{c,i}(t) \leq \overline{P}_{c,i} \quad (27)$$

$$\underline{Q}_{c,i} \leq Q_{c,i}(t) \leq \overline{Q}_{c,i} \quad (28)$$

$$\underline{P}_{p,i} \leq P_{p,i}(t) \leq \overline{P}_{p,i}(t) \quad (29)$$

$$\underline{Q}_{e,i} \leq Q_{e,i}(t) \leq \overline{Q}_{e,i} \quad (30)$$

2.5. Resilience Assessment Model

The flowchart of the proposed framework is shown in Figure 3. First, the distribution system to be studied is defined. The load demand, line parameters, protection settings, DER ratings and all other associated input data for the system and its components are obtained. As mentioned before, the study in this paper considers two types of strategies, (i) long-term infrastructural planning and (ii) short-term operational strategy. A strategy to be studied is chosen, and changes are made in the distribution system accordingly. For example, if the application of pole hardening is to be studied, changes are made in the parameters of structural fragility for the simulation. The graph network of the distribution system is generated to facilitate an efficient damage assessment model. An extreme wind event as discussed in Section 2.1 is generated. The damage assessment due to the extreme wind is conducted using Equations (3)–(5). The restoration of the affected load points takes place after the extreme wind subsides. The restoration time is calculated from Figure 2 and the restoration profile for the system is obtained as described in Section 2.3.

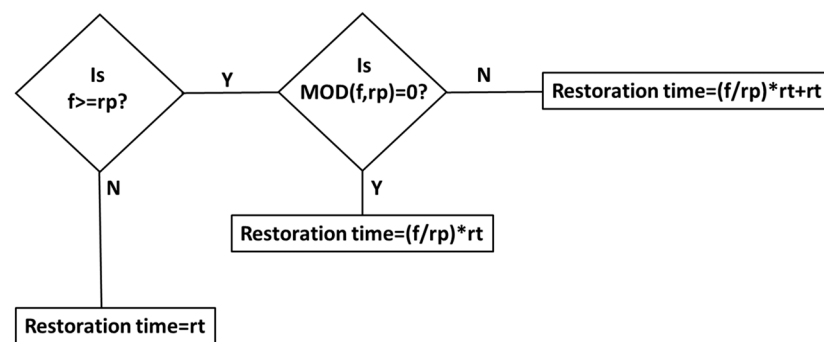


Figure 3. Logic diagram for restoration time.

A non-sequential Monte Carlo simulation-based program is developed in MATLAB to simulate the extreme event and perform the resiliency evaluation for different strategies. The load profile for the system before, during and after an event is obtained. The resiliency metrics are then evaluated based on the load profile of the system and the mitigating effects of the remedial strategies are observed and analyzed.

3. Application of the Proposed Resiliency Framework

When an extreme wind event occurs, the distribution network operators try to manage the resources available to them with the aim of minimizing load lost, considering options with the least economic stress. The availability of these resources during an event depends on the prior resilience planning of the system. The different investment decisions will result in different resilience performance of the system as the various resilience metrics are impacted in different ways. The following sections investigate different investment options and strategies to improve distribution system resiliency and present case studies. The extreme wind impact studies are carried out on the IEEE 69-bus test system shown in Figure 4.

The nominal voltage of the test system is 12.66 kV and the total load is 3.80 MW and 2.69 MVAR. The critical loads comprise 1.02 MW and 0.72 MVAR and their locations are shown in the Figure 4. The acceptable bus voltage range is set as 0.9 p.u. to 1.05 p.u. The distribution system has 400 kW of conventional generation, as shown in Table 2. As emerging environmental policies inhibit distributed power generation from fossil fuels, this study considers the integration of photovoltaics and battery storage at the network nodes shown in Figure 4. The DER integration complies with IEEE standard 1547 [26] and the ratings are given in Table 2. The charging and discharging efficiency of the ESS is taken as 0.95 each, and the rated discharge duration is 6 h. Advance notice of extreme winds are generally available with reasonable time to allow some degree of preparedness, such as storing energy in the ESS connected to the system. The initial SOC of the ESS is

therefore assumed to be 80% of the rated capacity. It is assumed that the DERs form the largest possible microgrid and the protective devices accordingly facilitates the formation of the microgrid. The reactive power limit for the CDG and ESS are assumed to be $\pm 70\%$ of the rated MW capacity. The operational cost of conventional DG is \$0.28/kWhr [17]. The operational cost associated with the PV and ESS are neglected. Penalty costs of \$500/MWhr and \$200/MWhr are used for critical and non-critical loads, respectively.

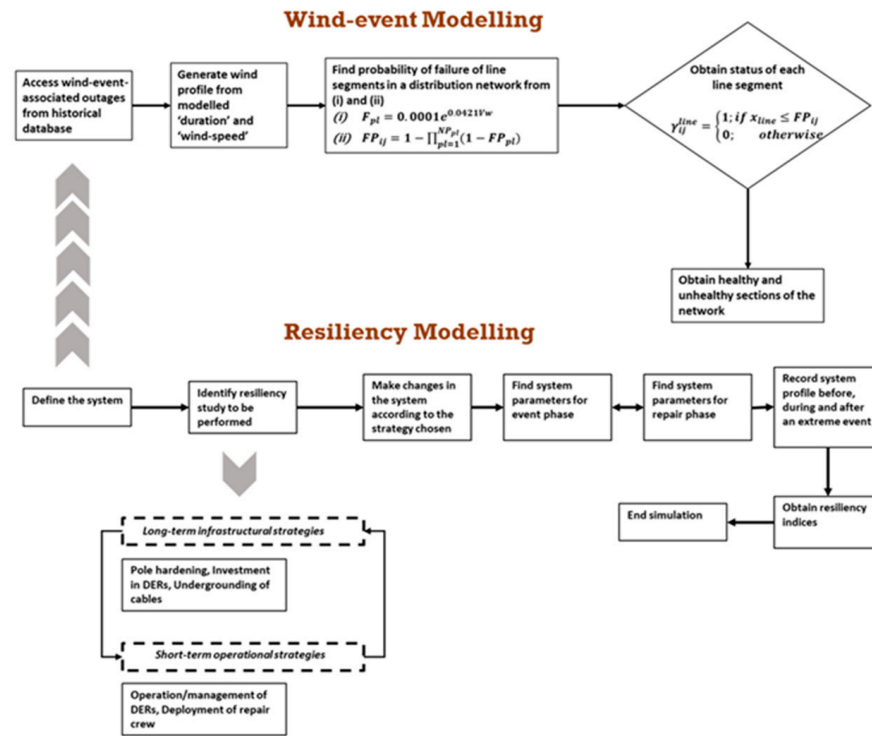


Figure 4. Flowchart of the proposed framework.

Table 2. Details of DERs used in the network.

Type of DERs	Bus No.	Rated Capacity (kW)
ESS	13 and 24	150
	46	75
	47	400
	54	50
PV	13 and 24	150
	36	75
	49	200
CDG	54	50
	20	100
	34	50
	64	250

An extreme wind profile is generated using Equations (1) and (2). Wind speed samples are generated using the MATLAB function 'evinv'. The average wind speed for extreme wind is taken as 58 mph, with the scaling parameter of 8 mph for the Gumbel distribution. The duration of the extreme wind event is randomly generated for each simulation.

A program was developed based on a non-sequential Monte Carlo simulation implemented in MATLAB R2019a. The program was used for data analysis and resiliency index calculation in the following studies.

3.1. Infrastructural Resiliency Assessment

3.1.1. Impact of Pole Hardening on Distribution System Resiliency

This section investigates the distribution system resiliency due to change in infrastructure hardness, mainly the fragility of the distribution system poles that support the overhead lines. These poles can have different structure design, such as single-pole or H-frame, and can be made from different materials, such as wood, steel or concrete. The different types of distribution poles and their erection are implemented using established utility practices that often follow IEEE standard C135.90-2014 [27]. The different designs and materials have different fragilities and show different levels of resilience in the case of an extreme event.

When the distribution poles are exposed to high winds, the withstanding capacity of the poles depends on their structural integrity. Some of the poles succumb to the strong winds and fall down, whereas others may not. The number of damaged poles depends on the wind speed and the structural integrity of the material used to construct the poles. The lines supported by the damaged poles cannot supply the load, and the system suffers load loss. The different levels of resiliency shown by the poles and their collective impact on the resiliency of the distribution system is examined by facilitating different cases studies. Case B considers the distribution lines supported by routinely maintained wooden poles, and is considered the base case study. Case A assumes a case where the wooden poles are not routinely maintained due to budget constraints, and therefore are exposed to considerable wear and tear over the years. The poles are assumed to be 30% more fragile than in the base case. Case C assumes the distribution system has steel poles due to investment in infractural hardness. The poles are assumed to be 30% more robust than in the base case. Figure 5 shows the fragility curves for the three cases. The fragility curves are mathematically expressed in Equation (31).

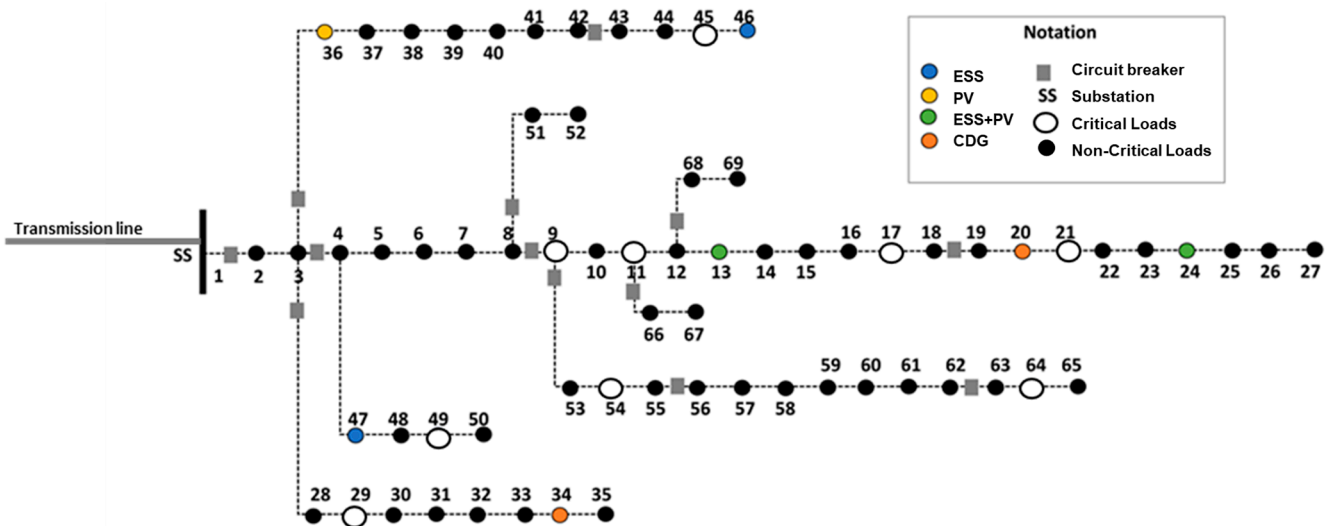


Figure 5. IEEE 69-bus test distribution network.

This study assumes the test system in Figure 4 does not include the DERs. The mean time to repair for each line segment in the distribution network is assumed to be 5 h. It is assumed that 20 crewmen are available for repair.

$$p_{f,dist_pole}(W_s = x_i) = 0.0001e^{0.0421x_i} \tag{31}$$

Figure 6 represents the resilience profile of the test system for cases A, B and C. It can be seen that the resilience profile obtained closely resembles the characteristics of the resilience trapezoid in Figure 1. Figure 6 shows that all three cases succumb to the extreme wind event and follow similar degradation profiles until the wind subsides. Case C, however, has the least number of poles damaged, and therefore, recovers faster than the other two cases. Case A has distribution poles with the weakest fragility curve, and therefore shows the poorest performance among the three cases in restoring the system. The effectiveness of the load restoration strategy as discussed in Section 2.3 is also verified, as critical loads are restored first, followed by the non-critical loads.

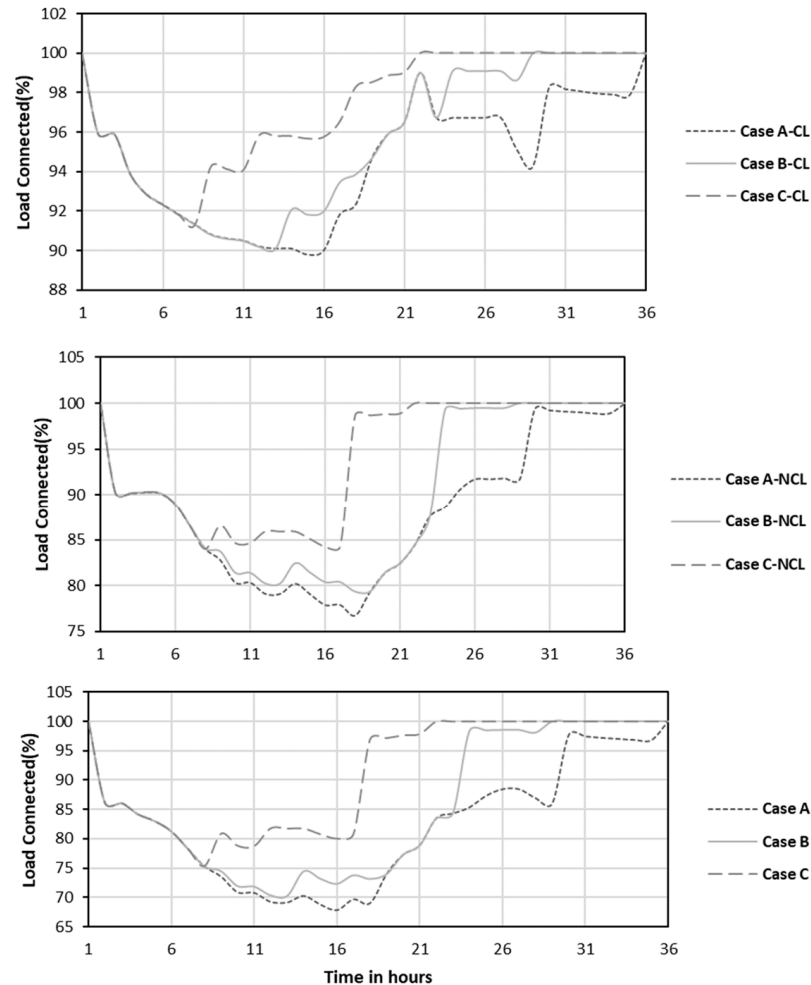


Figure 6. Resilience profile for cases A, B and C.

It should be noted that extreme winds with high peaks are less probable than extreme winds with moderate peaks. Another study was conducted to compare the resiliency of cases B and C, in which the extreme wind event peaks at 30 mph. The resilience profiles for the two cases are shown in Figure 7. In contrast to the previous study, the degradation in Phase I of the resilience profile is not the same for the two cases when the extreme wind is slightly moderate. The figure shows that the steel poles in Case C are able to withstand and ride through the event up to a certain point and degrade less severely than Case B with the wooden poles. The restoration in Case C is much faster than Case B due to fewer failures in system elements. The results from these studies provide evidence that investment in using proper guide wires to increase the strength of the poles or using stronger materials for the distribution poles can help achieve a more resilient distribution grid.

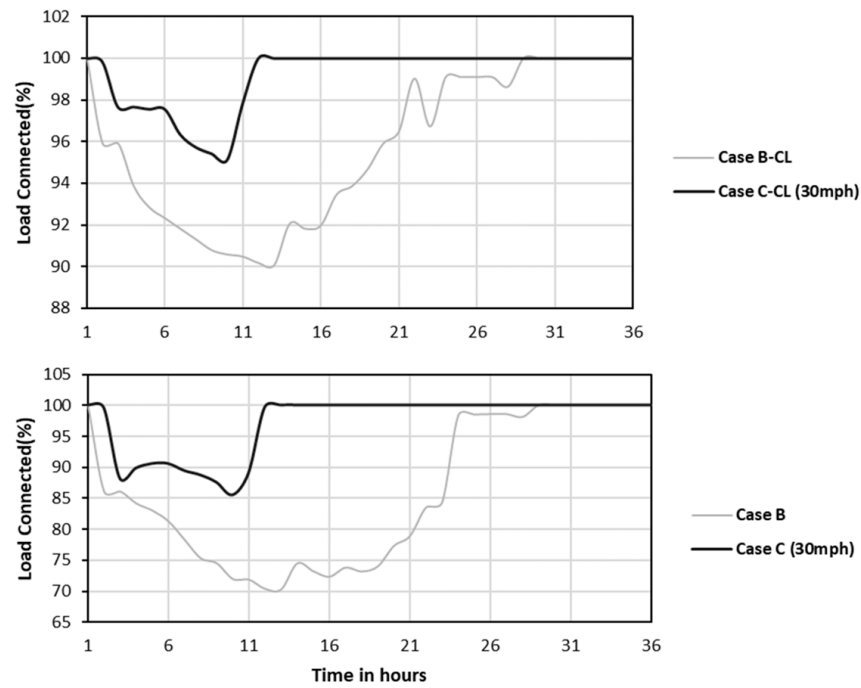


Figure 7. Resilience profiles for different wind speeds.

Figure 8 shows the response in terms of loads lost per hour of critical loads considering the materials of different structural fragility of the distribution poles during extreme wind. The figure shows that the poorer the fragility of the poles, the faster the load is lost in an extreme wind. This is because poor structural fragility increases the number of failed poles, increasing the number of failed lines in a distribution system, which translates to load loss in those areas. Case C (30 mph) refers to Case C in which the extreme wind peaks at 30 mph and experiences the slowest load loss of the cases. This is because a very small number of poles are damaged, as most of them ride through the extreme event. The results show that hardening poles is a preventive strategy that ensures a resilient distribution network.

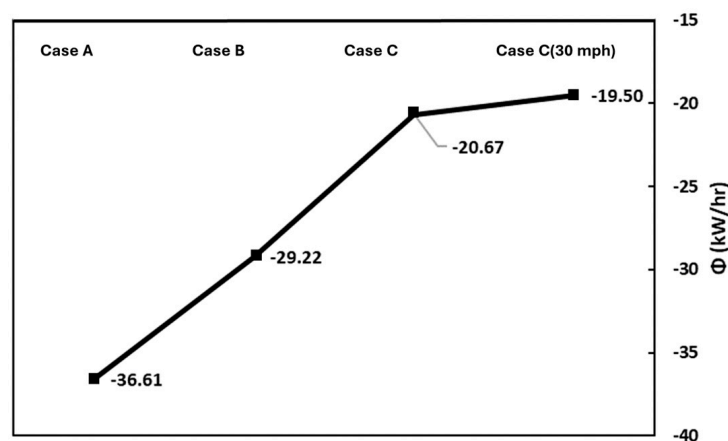


Figure 8. Φ response of different cases in event phase.

3.1.2. Impact of Repair Resources on Distribution System Resiliency

Repair personnel repair the damaged poles, line segments and other components and restore the load in the system. The impact of the availability of repair personnel on distribution system resiliency against extreme wind is investigated by carrying out three case studies on the test system. Cases B, D and E consider 20, 5 and 100 repair personnel,

respectively. Case E envisions a national rapid response team that can be immediately dispatched to locations that are under the threat of extreme wind events. Figure 9 shows the resilience profile of the distribution network for the three cases.

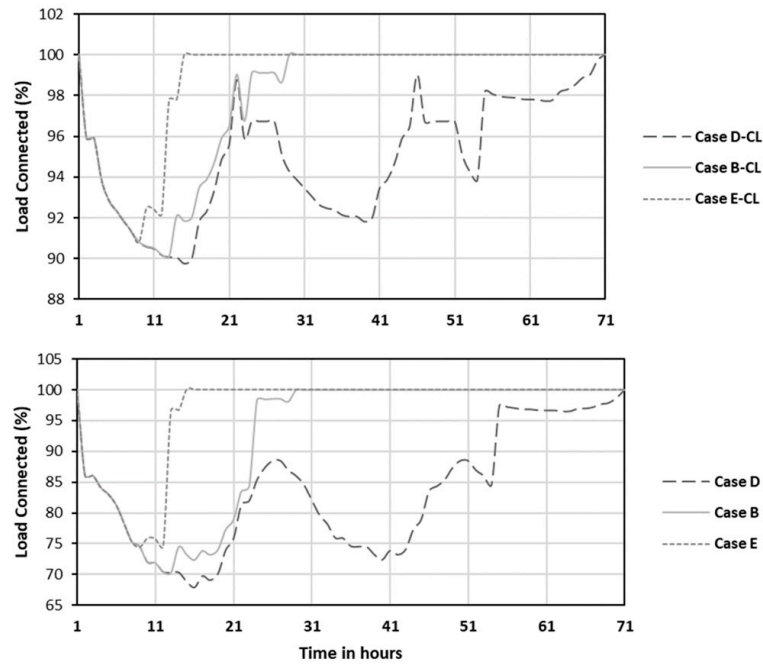


Figure 9. Resilience profile for cases D, B and E.

Case E has the best resilience profile of all three cases. Case D shows the worst performance, as case D is assumed to have the least amount of repair personnel. Increasing the number of repair personnel decreases the restoration time of the system. The second and third dips observed are due to the load profile for the second day, as the extreme event lasted for more than 24 h. Figure 9 shows that the recovery of the network can be greatly improved if the needed amount of repair personnel can be made available. Figure 10 shows the recovery rates, Π (kW/h) of all three cases. The results of Figure 10 show that Case E makes the fastest recovery of the three cases. A rapid response team filled with repair personnel should prove to be an efficient operational strategy against extreme winds.

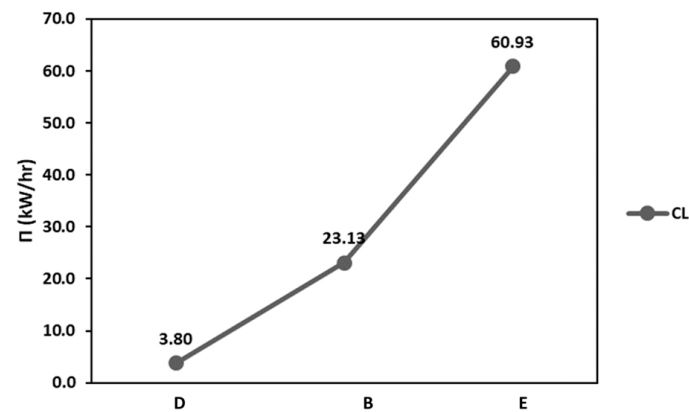


Figure 10. Π (kW/hr) for cases D, B and E.

Table 3 shows the EENS (MWhr/int) summarizing all of the cases involving infrastructural recovery strategies.

Table 3. EENS (MWhr/int) for different infrastructural recovery strategies.

Cases	EENS (MWhr/int)
A	54.64
B	39.41
C	24.41
D	59.38
E	35.53

Among the different infrastructural measures, using materials of higher structural fragility for distribution poles shows the least amount of energy lost. The results associated with the number of repair personnel quantifies the benefits of hiring additional personnel and can be used to make hiring decisions.

While the study results from the implementation of different remedial strategies improves the resilience of the distribution network, it is important to consider the scope of the strategies discussed. Case E aims to improve resiliency by providing better response strategies, but does not provide a scenario where the network can withstand an extreme event. Case C provides results to show that investment in using materials of higher structural fragility is an effective proactive strategy, and provides scenarios where the system is unaffected by extreme winds of lower intensities which in fact are more probable in occurrence. Case E is not proactive in nature, and is a corrective strategy, while case C is a preventive strategy. Each strategy has a different response from the system, and therefore, it is important to make balanced investment decisions to ensure a resilient distribution network. It is often difficult to justify an investment for resiliency because there is a high probability that the rare event will not occur during the lifetime of that investment. The proposed method, however, enables the planner to quantify and compare the benefits of investments in the different resilience enhancement strategies discussed above to make sound investment decisions.

3.2. Operating Strategies with DERs

This section assesses the change in resiliency of the system with the application of DERs. DERs form microgrids where possible, and ensure continuity of power when the power from the utility supply fails. In this way, DERs help in restoring power to the isolated section of the network, reducing the overall load lost in the system. In this study, case F is facilitated with DERs in the network that form an islanded microgrid when possible. The type of DERs present and the power supplied is given in Table 1. Case F is compared with the base case, Case B, which does not include DERs. The result shown in Figure 11 shows that the system incorporating DERs has a better resiliency profile than the system with no DERs in place. Figure 12 shows the recovery rate, Π (kW/h), for the two cases.

Figure 12 also agrees with the conclusions made from Figure 11. The system with DERs shows faster restoration than the system with no DERs in place. DERs also make the system independent and increase the flexibility of the system, as they ensure a continuous supply of load if the transmission line fails. DERs can be an effective strategy that provides a faster response to the system that has succumbed due to extreme winds, ensuring load-supply-forming microgrids.

A network with DERs has the fastest recovery of all of the cases, suggesting that networks with DERs are more resilient than others. However, the inclusion of DERs in a network requires an additional financial burden to the authorities that can sometimes outweigh the benefits of having DERs. It should, however, be noted that the DERs can only supply power to the load points if the poles and lines responsible for the power delivery are intact. It is therefore important to have a proper balance in the investment in DERs and in pole hardening. Studies such as those presented in this paper can be carried out on the system to determine the impacts of such investments and make a rational decision. The

investment in pole hardening alone cannot mitigate power outages from extreme wind events if the upstream transmission feeders are not hardened for the same objectives.

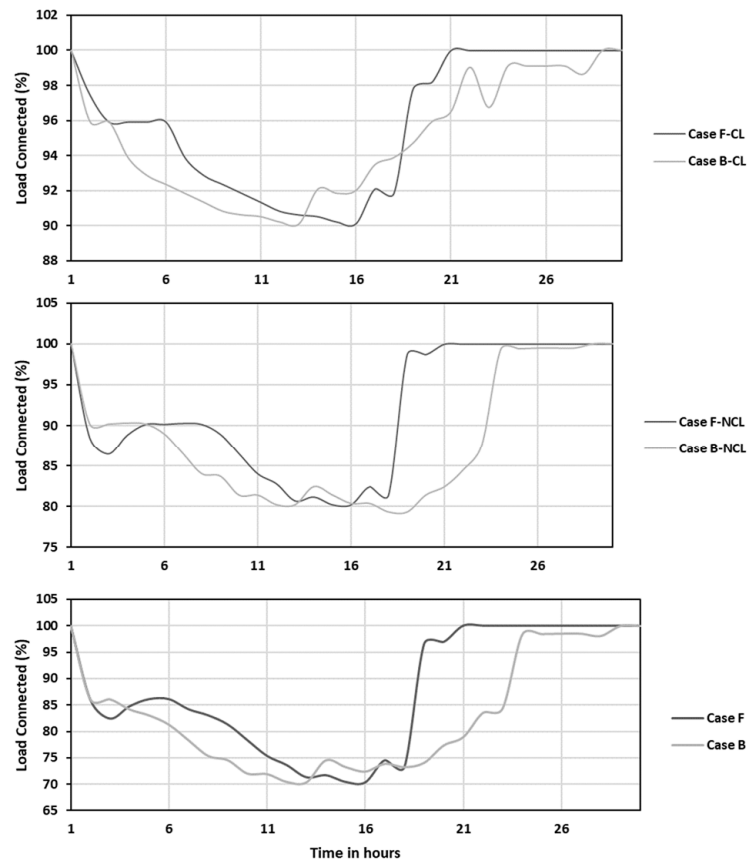


Figure 11. Resilience profiles for cases F and B.

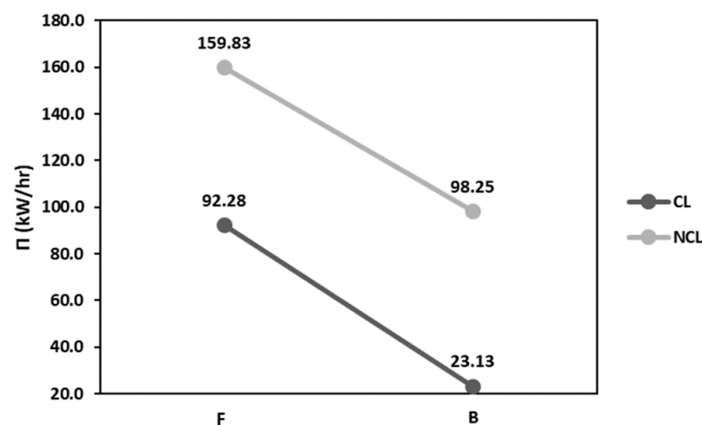


Figure 12. Π (kW/hr) for cases F and B.

3.3. Transmission Line Fragility and Its Impact on Distribution System Resiliency

A resilient distribution network will not suffice if the transmission network is not resilient enough against extreme winds. It is therefore important to consider the impact of transmission line fragility on distribution system resiliency. The upstream transmission line feeding the test system is shown in Figure 4. The transmission lines in the vicinity of the distribution system would also be exposed to the extreme wind event that affects the distribution system. The scope of this study is to understand the impact of the fragility of the transmission line on the distribution system.

This section models the fragility of transmission network poles using an empirical equation derived from [5]. Equation (32) gives the equation for structural fragility of the transmission network poles, where x_i is assumed to be the wind speed at any duration of time for which the failure probability of the pole is to be obtained.

$$p_{f,txn}(W_s = x_i) = 2 \times 10^{-7} e^{0.0834x_i} \quad (32)$$

The study considers two cases. Case B-txn is the base case considering the exposure of the transmission line to the extreme events. Case G assumes that the poles are 30% more fragile due to lack of maintenance from wear and tear. Figure 13 shows the resilience profiles of the network in the two cases.

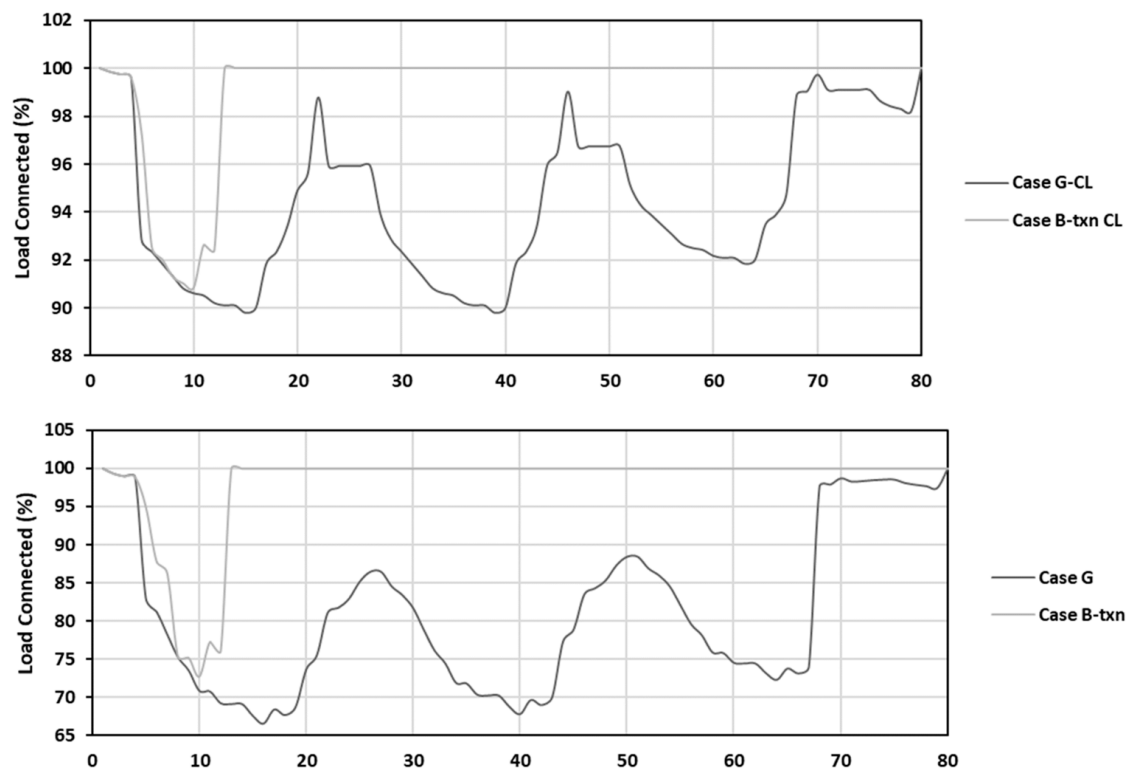


Figure 13. Resilience profiles for cases I and B.

Table 4 shows that a large amount of energy is lost in a system with poor transmission line fragility.

Table 4. EENS (MWhr/int) for Case I and B-txn.

Cases	EENS (MWhr/int)
G	66.67
B-txn	46.58

The drastic change in profiles in both the cases is due to very poor fragility of poles in Case G. This shows that the improvement in resiliency of the distribution system is not guaranteed if the fragility of the transmission network supplying power to the distribution network is poor. In this case, a distribution system equipped with DERs can restore power to the distribution system loads until the transmission lines are restored.

4. Conclusions

Extreme winds are one of the most frequently occurring extreme events threatening power distribution systems and are responsible for prolonged outages. This paper presents a resiliency assessment framework against extreme winds and explores various resiliency enhancement strategies.

This paper illustrates the application of the proposed framework on the IEEE 69-bus test system to assess the resiliency impacts of implementing a number of remedial strategies both at the planning and the operational phases. If sufficient investment for resiliency is made in the planning phase, the operating phase can avail the installed resources to mitigate the losses from the extreme wind event. If sufficient investment in pole hardening is made using materials of higher structural integrity such as steels, then it was found that the network could easily ride through wind storms of lower intensities and bear minimal damages to the network during wind storms with higher intensities. Also, this paper recommends the implementation of a ‘rapid response unit’ that consists of repair personnel ready to be deployed after an extreme wind event has occurred, as the results showed significant improvement in system down time when such units were deployed. This paper also shows that, if significant investment in DERs can be made in the planning phase, then considerable load loss can be minimized, and system down time can be reduced by deploying DERs in the operating phase. It was also found that the investment in DERs must also be accompanied with investment in selected pole hardening in order to deliver the distributed energy to the critical and non-critical loads in that priority order. This paper also explores the dependency of the distribution network on the structural strength of transmission lines, and finds that the resiliency of the distribution network cannot be guaranteed without a holistic approach that uses policies and frameworks to incorporate strategies that strengthen both the transmission and distribution networks. The distribution systems fed from fragile transmission networks can benefit significantly from investment in DERs, as the decisions on transmission system investments are outside the reach of distribution system owners.

Preventive strategies such as pole hardening help the network ride through extreme events with minimum damages, but do not provide any support when the structural integrity of the transmission network supplying the power to the grid is weak. Corrective strategies such as deployment of DERs do not provide the ability to withstand the extreme events, but provide rapid restoration to the network. Moreover, the deployment of DERs increases the independence of the network on the structural fragility of the transmission line supplying power to the network. Each strategy has a different response, and each strategy must be devised according to the need of the network, so this paper recommends balanced investment decisions to ensure a resilient distribution network. It is believed that the studies as presented in this paper can be carried out on a distribution system of interest to determine the impacts of such investments and make a rational decision.

Author Contributions: Conceptualization, methodology, R.K. and B.A.; software, validation, formal analysis, investigation, resources, data curation, writing—original draft preparation, B.A.; writing—review and editing, visualization, supervision, project administration, funding acquisition, R.K. All authors have read and agreed to the published version of the manuscript.

Funding: This research was funded by Natural Science and Engineering Research Council of Canada, Discovery Grant, RGPIN-2020-04477.

Data Availability Statement: The original contributions presented in the study are included in the article, further inquiries can be directed to the corresponding author.

Conflicts of Interest: The authors declare no conflict of interest.

References

1. Campbell, R.J.; Lowry, S. *Weather-Related Power Outages and Electric System Resiliency*; Congressional Research Service, Library of Congress: Washington, DC, USA, 2012.
2. Li, Z.; Shahidehpour, M.; Aminifar, F.; Alabdulwahab, A.; Al-Turki, Y. Networked microgrids for enhancing the power system resilience. *Proc. IEEE* **2017**, *105*, 1289–1310. [[CrossRef](#)]
3. Holling, C.S. Resilience and stability of ecological systems. *Annu. Rev. Ecol. Syst.* **1973**, *4*, 1–23. [[CrossRef](#)]
4. Watson, J.P.; Guttromson, R.; Silva-Monroy, C.; Jeffers, R.; Jones, K.; Ellison, J.; Rath, C.; Gearhart, J.; Jones, D.; Corbet, T.; et al. *Conceptual Framework for Developing Resilience Metrics for the Electricity Oil and Gas Sectors in the United States*; Technical Report; Sandia National Laboratories: Albuquerque, NM, USA, 2014.
5. Ouyang, M.; Duenas-Osorio, L. Multi-dimensional hurricane resilience assessment of electric power systems. *Struct. Saf.* **2014**, *48*, 15–24. [[CrossRef](#)]
6. Gao, H.; Chen, Y.; Xu, Y.; Liu, C.C. Resilience-oriented critical load restoration using microgrids in distribution systems. *IEEE Trans. Smart Grid* **2016**, *7*, 2837–2848. [[CrossRef](#)]
7. Farzin, H.; Fotuhi-Firuzabad, M.; Moeini-Aghtaie, M. Enhancing power system resilience through hierarchical outage management in multi-microgrids. *IEEE Trans. Smart Grid* **2016**, *7*, 2869–2879. [[CrossRef](#)]
8. Ma, S.; Su, L.; Wang, Z.; Qiu, F.; Guo, G. Resilience enhancement of distribution grids against extreme weather events. *IEEE Trans. Power Syst.* **2018**, *33*, 4842–4853. [[CrossRef](#)]
9. Panteli, M.; Mancarella, P.; Trakas, D.N.; Kyriakides, E.; Hatziaargyriou, N.D. Metrics and quantification of operational and infrastructure resilience in power systems. *IEEE Trans. Power Syst.* **2017**, *32*, 4732–4742. [[CrossRef](#)]
10. Panteli, M.; Trakas, D.N.; Mancarella, P.; Hatziaargyriou, N.D. Boosting the power grid resilience to extreme weather events using defensive islanding. *IEEE Trans. Smart Grid* **2016**, *7*, 2913–2922. [[CrossRef](#)]
11. Panteli, M.; Pickering, C.; Wilkinson, S.; Dawson, R.; Mancarella, P. Power system resilience to extreme weather: Fragility modeling, probabilistic impact assessment, and adaptation measures. *IEEE Trans. Power Syst.* **2016**, *32*, 3747–3757. [[CrossRef](#)]
12. Yao, S.; Wang, P.; Zhao, T. Transportable energy storage for more resilient distribution systems with multiple microgrids. *IEEE Trans. Smart Grid* **2018**, *10*, 3331–3341. [[CrossRef](#)]
13. Arif, A.; Ma, S.; Wang, Z.; Wang, J.; Ryan, S.M.; Chen, C. Optimizing service restoration in distribution systems with uncertain repair time and demand. *IEEE Trans. Power Syst.* **2018**, *33*, 6828–6838. [[CrossRef](#)]
14. Yuan, W.; Wang, J.; Qiu, F.; Chen, C.; Kang, C.; Zeng, B. Robust optimization-based resilient distribution network planning against natural disasters. *IEEE Trans. Smart Grid* **2016**, *7*, 2817–2826. [[CrossRef](#)]
15. Xu, Y.; Liu, C.C.; Schneider, K.P.; Tuffner, F.K.; Ton, D.T. Microgrids for service restoration to critical load in a resilient distribution system. *IEEE Trans. Smart Grid* **2016**, *9*, 426–437. [[CrossRef](#)]
16. Yuan, C.; Illindala, M.S.; Khalsa, A.S. Modified Viterbi algorithm based distribution system restoration strategy for grid resiliency. *IEEE Trans. Power Deliv.* **2016**, *32*, 310–319. [[CrossRef](#)]
17. Wang, Z.; Wang, J. Self-healing resilient distribution systems based on sectionalization into microgrids. *IEEE Trans. Power Syst.* **2015**, *30*, 3139–3149. [[CrossRef](#)]
18. Poudel, S.; Dubey, A. Critical load restoration using distributed energy resources for resilient power distribution system. *IEEE Trans. Power Syst.* **2018**, *34*, 52–63. [[CrossRef](#)]
19. Bajpai, P.; Chanda, S.; Srivastava, A.K. A novel metric to quantify and enable resilient distribution system using graph theory and choquet integral. *IEEE Trans. Smart Grid* **2016**, *9*, 2918–2929. [[CrossRef](#)]
20. Mousavizadeh, S.; Haghifam, M.R.; Shariatkhah, M.H. A linear two-stage method for resiliency analysis in distribution systems considering renewable energy and demand response resources. *Appl. Energy* **2018**, *211*, 443–460. [[CrossRef](#)]
21. Chanda, S.; Srivastava, A.K. Defining and enabling resiliency of electric distribution systems with multiple microgrids. *IEEE Trans. Smart Grid* **2016**, *7*, 2859–2868. [[CrossRef](#)]
22. Gautam, P.; Piya, P.; Karki, R. Resilience assessment of distribution systems integrated with distributed energy resources. *IEEE Trans. Sustain. Energy* **2020**, *12*, 338–348. [[CrossRef](#)]
23. Bie, Z.; Lin, Y.; Li, G.; Li, F. Battling the extreme: A study on the power system resilience. *Proc. IEEE* **2017**, *105*, 1253–1266. [[CrossRef](#)]
24. Liu, Y.; Wang, Y.; Wang, Q.; Zhang, K.; Qiang, W.; Wen, Q.H. Recent advances in data-driven prediction for wind power. *Front. Energy Res.* **2023**, *11*, 1204343. [[CrossRef](#)]
25. Mukherjee, S.; Nateghi, R.; Hastak, M. Data on major power outage events in the continental US. *Data Brief* **2018**, *19*, 2079–2083. [[CrossRef](#)] [[PubMed](#)]
26. *IEEE Std 1547-2018*; IEEE Standard for Interconnection and Interoperability of Distributed Energy Resources with Associated Electric Power Systems Interfaces. IEEE: Piscataway, NJ, USA, 2018. [[CrossRef](#)]
27. *IEEE Std C135.90-2014*; IEEE Standard for Pole Line Hardware for Overhead Line Construction. IEEE: Piscataway, NJ, USA, 2014. [[CrossRef](#)]

Disclaimer/Publisher’s Note: The statements, opinions and data contained in all publications are solely those of the individual author(s) and contributor(s) and not of MDPI and/or the editor(s). MDPI and/or the editor(s) disclaim responsibility for any injury to people or property resulting from any ideas, methods, instructions or products referred to in the content.